

Calcium Transients Modulate Action Potential Repolarizations in Ventricular Fibrillation

Bum-Rak Choi, Tong Liu, and Guy Salama

Abstract— Action potential alternans has been an indicator of ischemic disease and vulnerability to ventricular fibrillation (VF). The mechanisms of alternans are linked to the anomalies in intracellular Ca^{2+} (Ca_i) handling by either spontaneous Ca^{2+} release or modulation of action potential duration (APD), which may promote wave breaks in VF. We investigated possible role of Ca^{2+} in wave breaks by simultaneously measuring transmembrane potential (V_m) and intracellular Ca^{2+} concentration with voltage sensitive dye (RH237) and Ca^{2+} (Rhod-2) fluorescence probes. VF was induced by burst stimulation and the relationship between V_m and Ca^{2+} oscillations in VF were analyzed with cross-correlation analysis. The maximum correlation occurred at 12 ms delay between V_m and Ca_i , suggesting V_m still triggers Ca^{2+} release in VF as in normal excitation-contraction coupling. In addition, inverse correlation was found -20 ms between V_m and Ca_i , suggesting the amplitude of Ca_i can modulate action potential recovery in VF. In conclusion, Ca_i can influence action potential durations, which may promote wave breaks in VF.

I. INTRODUCTION

CALCIUM is an important regulator of the normal physiological function including muscle contraction, the activation and regulation of various enzymes, metabolic pathways, and the control of gene transcription factors. Among those, the heart uses Ca^{2+} to accomplish a synchronized muscle contraction via excitation-contraction coupling (EC coupling) and intracellular Ca^{2+} concentration (Ca_i) is tightly regulated during cardiac beats. Defects in these processes have been linked to cardiac arrhythmias by altering excitability of cardiac tissue [1].

In general, the onset of fibrillation is linked to the development of spiral waves (reentrant activation). The possibility of unidirectional propagation and subsequent reentry by premature stimuli increases when repolarization occurs heterogeneously across the heart. Once formed, spiral waves may meander, drift, anchor, or break up into multiple spirals, depending on tissue characteristics [2].

Spiral waves may be unstable and tend to breakup into turbulence. To induce wave breakups, not only dispersion of

repolarization but also the dynamical properties of action potential duration (APDs) may play important roles (restitution hypothesis [3]). APD restitution is a measure of APD shortening as a function of diastolic intervals (DIs). When the slope of APD restitution curve is above 1, small APD oscillations such as alternans can progress into bigger APD oscillations and eventually wave breakups occur [4].

The Ca^{2+} handling has been implicated as a trigger of electrical alternans [5-9], in which the amplitude and/or the duration of APs alternate between odd and even beats. In this hypothesis, intracellular Ca^{2+} cycling does not recover as rapidly as APs so that after full size of Ca^{2+} release, next Ca^{2+} release can be premature and smaller in size. Ca^{2+} alternans may in turn promote APD alternans through various Ca^{2+} currents including L-type Ca^{2+} current (I_{Ca}), Na^+ - Ca^{2+} exchanger (I_{NaCa}), or calcium-sensitive Cl^- currents, eventually promote wave breaks in VF [10, 11]. In addition, Ca^{2+} elevation can reduce gap junction conductance and increase conduction blocks and reentry formation. However, the role of Ca^{2+} cycling in VF is still a matter of conjecture.

The objective of this study, therefore, was to investigate whether Ca^{2+} modulates APD in VF. V_m and Ca^{2+} were measured simultaneously using two fluorescence probes (RH237 and Rhod2) from the anterior region of guinea pig hearts. The correlation analysis of V_m and Ca^{2+} in VF shows the existence of inverse relationship between Ca^{2+} and action potential recovery, supporting the hypothesis that Ca^{2+} is an important modulator of action potentials in VF.

II. METHODS

A. Heart preparation

Guinea pigs (male, ~ 450 g, n=7) were injected with pentobarbital (45 mg/kg) plus heparin (200 U/kg), then the heart was excised and retrogradely perfused through the aorta with (in mM): 130 NaCl, 24 NaHCO_3 , 1.0 MgCl_2 , 4.0 KCl, 1.2 NaH_2PO_4 , 5 Dextrose, 45 mannitol, 1.25 CaCl_2 , at pH 7.4, gassed with 95 % O_2 and 5 % CO_2 . This investigation conformed to the current Guide for Care and Use of Laboratory Animals published by the National Institutes of Health (NIH Publication No. 85-23, revised 1996). Temperature was maintained at 37.0 ± 0.2 °C and perfusion pressure was adjusted to ~70 mm Hg with a peristaltic pump [12].

Hearts were stained with a voltage sensitive dye (RH 237, 10 μl of 1 mg/ml of dimethyl sulfoxide, DMSO) and were loaded with a Ca^{2+} indicator (Rhod 2/AM, 200 μl of 1 mg/ml DMSO) delivered through the bubble trap, above the aortic

Manuscript received Apr 1, 2006. This work was supported in part by the American Heart Association Beginning Grant-In-Aid awarded to B.-R. Choi and NIH ROI HL057929 and HL HL69097 to G. Salama.

B.-R. Choi was with University of Pittsburgh, Pittsburgh, PA 15261 USA. He is now with the department of Biomedical Engineering, Tulane University, New Orleans, LA 70118 USA (corresponding author to provide phone: 504-247-1911, fax: 504-862-8779 e-mail: bchoi@tulane.edu).

T. Liu is with University of Pittsburgh, Pittsburgh, PA 15261 USA. the National Institute of Standards and Technology, Boulder, CO 80305 USA (e-mail: tgl67@yahoo.com).

G. Salama is with University of Pittsburgh, Pittsburgh, PA 15261 USA. (e-mail: gsalama@pitt.edu).

cannula. EKGs and perfusion pressure were continuously monitored to insure that the dyes did not produce lasting pharmacological effects. Hearts were placed in a chamber to reduce movement artifacts.

B. Optical Apparatus

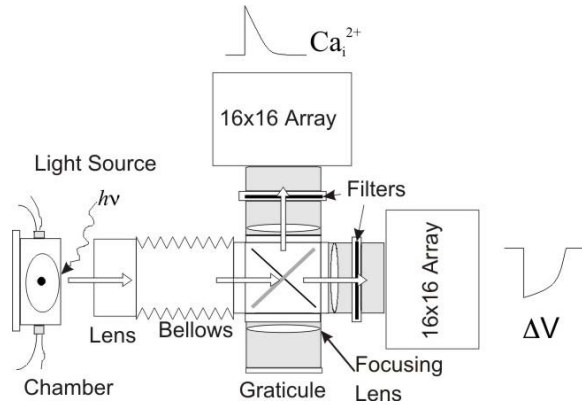


Fig. 1. Optical apparatus for simultaneous V_m and Ca_i recordings. Two Hamamatsu photodiode arrays are located at 90° angle to record fluorescence signals of Ca^{2+} and V_m from $13 \times 13 \text{ mm}^2$ of anterior region of heart.

The optical apparatus (Fig. 1) was previously described [12]. Briefly, light from two 100-W tungsten-halogen lamps was collimated, passed through $520 \pm 30 \text{ nm}$ interference filters, and fluorescence emitted from the stained heart was collected with a camera lens passed through a 45° dichroic mirror (630 nm cut-off, Omega Optical, Brattleboro, VT) to reflect the Rhod-2 fluorescence while transmitting the RH 237 fluorescence. Fluorescence images from each dye were pass through additional filters ($585 \pm 15 \text{ nm}$ and $> 715 \text{ nm}$ for Rhod-2 and RH 237 respectively) and refocused on two 16×16 photodiode arrays (Hamamatsu Corp. #C4675-103) such that each diode on the ‘voltage array’ was in exact register with a diode on the ‘calcium array’. Outputs from the arrays were amplified, digitized at 2000 frames/s and stored in computer memory.

C. Data Analysis

Cross correlation (CC) calculates correlation coefficient between two signals after shifting time lag [13]. The cross correlation of two signals, X and Y and time lag (L) was defined as

$$R_{XY}(L) = \begin{cases} \frac{\sum_{k=0}^{N-L-1} (X_{k+L} - \bar{X})(Y_k - \bar{Y})}{\sqrt{\sum_{k=0}^{N-1} (X_k - \bar{X})^2} \sqrt{\sum_{k=0}^{N-1} (Y_k - \bar{Y})^2}} & \text{For } L < 0 \\ \frac{\sum_{k=0}^{N-L-1} (X_k - \bar{X})(Y_{k+L} - \bar{Y})}{\sqrt{\sum_{k=0}^{N-1} (X_k - \bar{X})^2} \sqrt{\sum_{k=0}^{N-1} (Y_k - \bar{Y})^2}} & \text{For } L \geq 0 \end{cases}$$

Where \bar{X} and \bar{Y} are means of corresponding series and N is the number of points in the series. The maximum correlation between two occurs when two signals are nicely overlapped. The time delay and maximum correlation were calculated from at least 200 pixels and the data was

represented with mean and standard deviations.

III. V_m AND Ca^{2+} RELATIONSHIP

A. V_m and Ca_i under Normal Condition

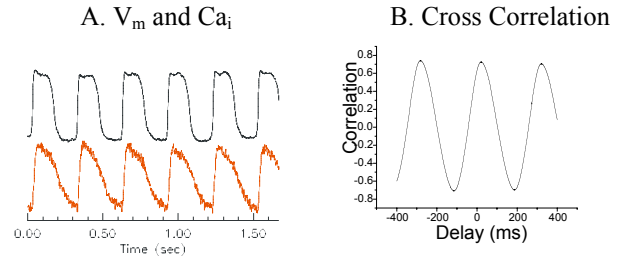


Fig. 2. Cross correlation between V_m (black) and Ca_i (red). (A) Hearts were stimulated at 300 ms cycle length and V_m (black line) and Ca_i (red line) were measured as described in the Methods. (B) Cross correlation analysis shows maximum correlation at $10.4 \pm 0.5 \text{ ms}$ which is compatible with time delay between V_m and Ca_i .

Figure 2 shows a typical example of V_m and Ca_i recordings from one of the pixels. The heart was stimulated at 300 ms basic cycle length from the right ventricle using a bipolar AgCl electrode. The rise of action potential always precedes the rise of Ca_i with time delay $10.4 \pm 0.5 \text{ ms}$, indicating normal excitation-contraction coupling where action potential triggers Ca^{2+} release from sarcoplasmic reticulum.

The cross correlation analysis between action potential and Ca_i of regular beats shows high correlation (>0.8) between V_m and Ca_i signals (Fig. 2B). The maximum correlation (CC_{\max}) between two occurred at the time lag of 10.4 ms, which is compatible with the time delay between action potential and Ca_i measured above, suggesting the correlation analysis can be used to quantify relationship between V_m and Ca_i . The high correlation (>0.8) between two under normal condition suggests very tight control of Ca_i by V_m . Note that the correlation between V_m and Ca_i reaches maximum (CC_{\max}) at basic cycle length of $\pm 300 \text{ ms}$. This is because the shape of action potential and calcium transients are stable beat to beat.

B. V_m and Ca_i during Ischemia

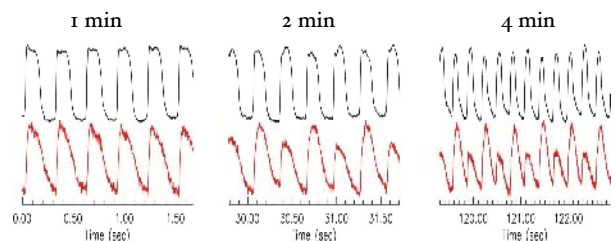


Fig. 3. V_m (top traces) and Ca_i (bottom traces) during ischemia. Note that the amplitudes of Ca_i alternate between odd and even beats.

We further investigated relationship between V_m and Ca_i under ischemic condition. Hearts were continuously stimulated at 300 ms cycle length from the right ventricle and the perfusion pump was stopped to cause global ischemia. During ischemia, the temperature of heart chamber

was maintained at 37 °C by a custom-built heater and feedback system.

Figure 3 shows V_m and Ca_i under ischemic condition. With progress of ischemia, the amplitude of Ca_i started alternating between odd and even beats. Alternans of V_m and

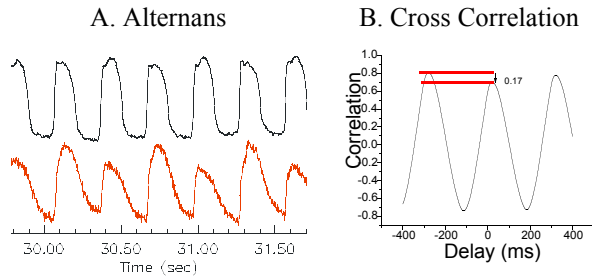


Fig. 4. CC_{max} and the time delay between V_m and Ca_i during ischemia. (A) Typical examples of alternans. (B) Cross Correlation between V_m and Ca_i traces in panel A. CC_{max} occurred when odd beats of action potentials are superimposed with even beats of Ca_i .

Ca_i can be analyzed using cross correlation analysis.

Figure 4 shows cross correlation of V_m and Ca_i . Unlike normal condition where CC_{max} occurred at the time delay between V_m and Ca_i , CC_{max} in ischemia occurred when V_m is shifted with the time lag of basic cycle length. This is because action potentials and Ca_i transients alternate between odd and even beats. The phase of alternans between V_m and Ca_i are discordant where larger action potentials are associated with smaller Ca_i transients. Therefore, the best overlap of two signals can be obtained when one signal is shifted about the basic cycle length where larger action potential can be correlated with larger Ca_i transient of following beat.

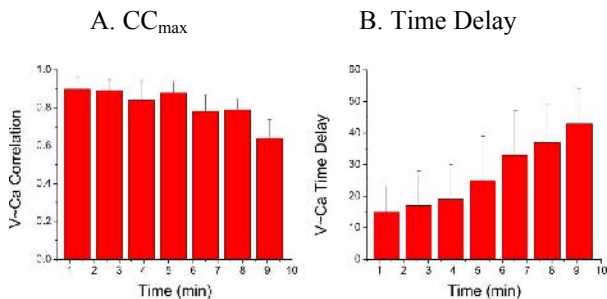


Fig. 5. CC_{max} and the time delay between V_m and Ca_i during ischemia. CC_{max} decreases while time delay of action potential and Ca_i increases, suggesting that the relationship between action potential and Ca_i is being disrupted by ischemia.

Figure 5 shows CC_{max} and time delay between action potential and calcium transients during ischemia. CC_{max} and the time delay between V_m and Ca_i during ischemia suggest that V_m and Ca_i lost their tight relationship compared to the normal condition (see Fig. 2 & 3).

C. V_m and Ca_i in VF

VF was induced by burst stimulation and V_m and Ca_i were simultaneously recorded as described in the Methods. Ca_i oscillations were still in synchrony with V_m oscillations as

shown Figure 6A. The time delay was 12 ms ($n=3$ hearts), which can be confirmed by overlapping two traces of V_m and Ca_i in Figure 6B middle panel.

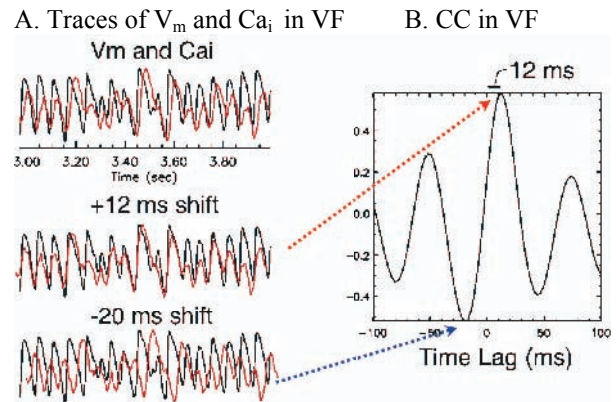


Fig. 6. Correlation and time delay between V_m and Ca_i in VF. (A) Typical example of V_m and Ca_i in VF. Two traces are well overlapped when V_m trace is shifted 12 ms (middle trace). (B) Correlation vs. time lag. The maximum correlation was associated with time delay between V_m and Ca_i as in Figure 1, suggesting action potential triggers Ca_i release in VF. Note that the inverse correlation can be also observed at -20 ms time lag, suggesting larger Ca_i causes smaller amplitude of following action potentials.

The time delay between action potential and Ca_i can be also shown in correlation plot (panel B). CC reaches at maximum when two traces are overlapped each other with time delay of 12 ms, suggesting V_m still triggers Ca_i release in VF.

We further investigated possible correlation between APD and Ca^{2+} in VF. Ca^{2+} can modulate APD in both positive and negative ways through Ca^{2+} dependent currents, Na^+/Ca^{2+} exchanger (I_{NaCa}) that depolarize V_m by elevation of Ca^{2+} , and L-type Ca^{2+} currents (I_{Ca}) that are inactivated by elevation of Ca^{2+} . As a result, Ca^{2+} can either prolong or shorten APD depending on relative magnitude and contribution of I_{NaCa} and I_{Ca} . We hypothesized that larger amplitude of Ca^{2+} may primarily accelerate inactivation of I_{Ca} and subsequently earlier repolarization. To verify this hypothesis, correlation of action potential repolarization phase and the amplitude of Ca^{2+} were investigated. We found that the correlation was negative at -20 ms time lag (see Figure 6A bottom trace and panel B). The negative correlation was due to the association between larger Ca_i and earlier repolarization of action potentials (Figure 6A lower panel), suggesting that Ca_i release influences the recovery and subsequent action potential amplitudes in VF.

IV. CONCLUSION

Electrical alternans has been linked to initiation and maintenance of VF by wave breaks, a hallmark of VF. As a mechanism of electrical alternans, Ca^{2+} cycling has been implicated through Ca^{2+} sensitive ion channels including I_{Ca} , I_{NaCa} and $I_{Cl,Ca}$. However, there is a lack of data regarding whether or how Ca_i cycling influences action potential durations. The present study investigated possible roles of

Ca_i in VF by simultaneously recording V_m and Ca_i from the epicardial surface of fibrillating hearts using fluorescence probes. The cross correlation analysis between action potential and Ca²⁺ transients showed a negative correlation, indicating that a larger Ca²⁺ transient may promote earlier action potential repolarization while smaller Ca²⁺ transient may prolong action potential repolarization. As a result, the instability in Ca²⁺ transients increases APD alternans, strongly supporting the hypothesis that Ca²⁺ cycling may be a major factor to modulate excitability of tissues in VF.

REFERENCE

- [1] M. Scoote and A. J. Williams, Myocardial calcium signalling and arrhythmia pathogenesis, *Biochem Biophys Res Commun*, vol. 322, pp. 1286-309, 2004.
- [2] J. Jalife, Ventricular fibrillation: mechanisms of initiation and maintenance, *Annu Rev Physiol*, vol. 62, pp. 25-50, 2000.
- [3] A. Karma, Electrical alternans and spiral wave breakup in cardiac tissue, *Chaos*, vol. 4, pp. 461-472, 1994.
- [4] R. F. Gilmour and D. R. Chialvo, Electrical restitution, critical mass, and the riddle of fibrillation, *J Cardiovasc Electrophysiol*, vol. 10, pp. 1087-1089., 1999.
- [5] D. E. Euler, Cardiac alternans: mechanisms and pathophysiological significance, *Cardiovasc Res*, vol. 42, pp. 583-90, 1999.
- [6] H. Bien, L. Yin, and E. Entcheva, Calcium instabilities in mammalian cardiomyocyte networks, *Biophys J*, vol. 90, pp. 2628-40, 2006.
- [7] W. T. Clusin, Calcium and cardiac arrhythmias: DADs, EADs, and alternans, *Crit Rev Clin Lab Sci*, vol. 40, pp. 337-75, 2003.
- [8] K. Hiromoto, H. Shimizu, Y. Furukawa, T. Kanemori, T. Mine, T. Masuyama, and M. Ohyanagi, Discordant repolarization alternans-induced atrial fibrillation is suppressed by verapamil, *Circ J*, vol. 69, pp. 1368-73, 2005.
- [9] M. L. Walker and D. S. Rosenbaum, Cellular alternans as mechanism of cardiac arrhythmogenesis, *Heart Rhythm*, vol. 2, pp. 1383-6, 2005.
- [10] E. Chudin, A. Garfinkel, J. Weiss, W. Karplus, and B. Kogan, Wave propagation in cardiac tissue and effects of intracellular calcium dynamics (computer simulation study), *Prog Biophys Mol Biol*, vol. 69, pp. 225-236, 1998.
- [11] E. Chudin, J. Goldhaber, A. Garfinkel, J. Weiss, and B. Kogan, Intracellular Ca(2+) dynamics and the stability of ventricular tachycardia, *Biophys J*, vol. 77, pp. 2930-2941, 1999.
- [12] B. R. Choi and G. Salama, Simultaneous maps of optical action potentials and calcium transients in guinea-pig hearts: mechanisms underlying concordant alternans, *J Physiol*, vol. 529, pp. 171-188, 2000.
- [13] B. R. Choi, T. Liu, M. Lavasani, and G. Salama, Fiber orientation and cell-cell coupling influence ventricular fibrillation dynamics, *J Cardiovasc Electrophysiol*, vol. 14, pp. 851-60, 2003.